

Landing Force Control for Humanoid Robot by Time-Domain Passivity Approach

Yong-Duk Kim, Bum-Joo Lee, Jee-Hwan Ryu, and Jong-Hwan Kim

Abstract—This paper proposes a control method to absorb the landing force or the ground reaction force for a stable dynamic walking of a humanoid robot. Humanoid robot may become unstable during walking due to the impulsive contact force of the sudden landing of its foot. Therefore, a control method to decrease the landing force is required. In this paper, time-domain passivity control approach is applied for this purpose. Ground and the foot of the robot are modeled as two one-port network systems that are connected, and exchange energy with each other. The time-domain passivity controller with admittance causality is implemented, which has the landing force as input and foot's position to trim off the force as output. The proposed landing force controller can enhance the stability of the walking robot from simple computation. The small-sized humanoid robot, HanSaRam-VII that has 27 DOFs, is developed to verify the proposed scheme through dynamic walking experiments.

Index Terms—Dynamic walking, humanoid robot, landing force control, time-domain passivity control.

I. INTRODUCTION

A humanoid robot is a bipedal (i.e., two-legged) robot, and is expected to eventually evolve into one with a human-like body. A lot of recent research has been focused on the development of humanoid robot that is similar to human beings, both morphologically and functionally [1]–[4]. Current research, being conducted in collaborating operations with human beings [5], [6], has progressed far beyond studies in walking trajectory generation [7]–[9] and online (real-time) balance control [10]–[12] during walking. Though walking pattern is made considering the ground reaction force, because of various errors such as errors of parts and delay of control, the ground reaction force does not act on the robot at expected time and in expected magnitude. Therefore, one of the essential research areas is the reduction of the landing force or the ground reaction force that is created between the foot and the surface during walking, and this paper aims to solve this challenge.

By far, there have been many researches to reduce landing force for walking or running humanoid robot. According to the methods, they can be classified into three categories:

- 1) Method using heuristic damping control.
- 2) Method using dynamic equation of a robot and its environment.
- 3) Method using unique structure of feet.

Huang and Nakamura got the information about the condition of the ground through force sensor, and modified offline pattern in real time using heuristic method [13]. Also, Kajita *et al.* introduced a method of a sort of damping control; if foot lands on the ground, it is

Manuscript received January 31, 2007. This paper was recommended for publication by Associate Editor Q. Huang and Editor H. Arai upon evaluation of the reviewers' comments.

Y.-D. Kim, B.-J. Lee, and J.-H. Kim are with the Department of Electrical Engineering and Computer Science, Korea Advanced Institute of Science and Technology (KAIST), Daejeon 305-701, Korea (e-mail: ydkim@rit.kaist.ac.kr; bjlee@rit.kaist.ac.kr; johkim@rit.kaist.ac.kr).

J.-H. Ryu is with the School of Mechanical Engineering, Korea University of Technology and Education, Cheonan 330-708, Korea (e-mail: jhryu@kut.ac.kr).

This paper has supplementary downloadable material available at <http://ieeexplore.ieee.org>, provided by the authors. This includes two multimedia wmv format movie clips, which show the experimental results. This material is 7.99 MB in size.

Color versions of one or more of the figures in this paper are available online at <http://ieeexplore.ieee.org>.

Digital Object Identifier 10.1109/TRO.2007.906250

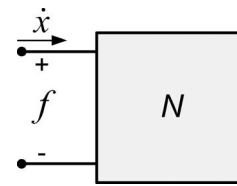


Fig. 1. One-port network model.

moved up in a constant velocity [14]. Likewise, there was a research in order to change foot's position using several control method [15], [16]. These are easy to implement, but they are troublesome in that damping coefficient or PID control coefficients should be determined manually through trial and errors.

On the other hand, there was a research to reduce landing force using hybrid impedance control method or computed torque control after solving the dynamic equation of robots and the environment [17]–[19]. In this case, control parameter can be calculated mathematically. However, not only complicated dynamic equation has to be calculated, but also sometimes control parameter should be regulated according to the walking condition. Also, there was a research to reduce landing force physically by using unique feet structure [20].

This paper proposes a novel method to compensate for the landing force of a humanoid robot. The method is based on time-domain passivity approach [21]–[24], where the robot's foot is modeled as a one-port network system with admittance causality (the landing force is an input and foot's position is an output). By calculating the energy input into the one-port network based on the landing force and the foot position, the robot's foot is controlled to be passive. The method does not need a complex and special foot structure. In addition to this, because it does not need any parameters to be tuned, effort to determine the damping coefficient is unnecessary, and also, exact control can be accomplished. The validity of the proposed control method is confirmed through dynamic walking experiments using the small-sized humanoid robot, HanSaRam-VII developed at RIT Laboratory, Korea Advanced Institute of Science and Technology (KAIST), in 2006.

The remainder of this paper is organized as follows. In Section II, time-domain passivity is briefly reviewed. Section III describes the modeling of robot's foot system that consists of robot's foot and ground surface. In Section IV, the time-domain passivity control to compensate for the landing force is proposed. Section V explains the real implementation of humanoid robot and presents the three experimental results with the conventional damping control method and with and without the proposed method for comparison. Finally, conclusions follow in Section VI.

II. REVIEW OF THE TIME-DOMAIN PASSIVITY

In this section, we briefly review time-domain passivity concept before it is implemented for absorbing the landing force. First, we define the sign convention for all forces and velocities so that their product is positive when power enters the system port. Also, the system is assumed to have initial stored energy at $t = 0$ of $E(0)$ (Fig. 1). The following widely well-known definition of passivity is then used.

Definition 1: The one-port network N with initial energy storage $E(0)$ is continuous time passive if and only if

$$E(t) = \int_0^t f(\tau)\dot{x}(\tau) d\tau + E(0) \geq 0 \quad \forall t \geq 0 \quad (1)$$

for force f and velocity \dot{x} .

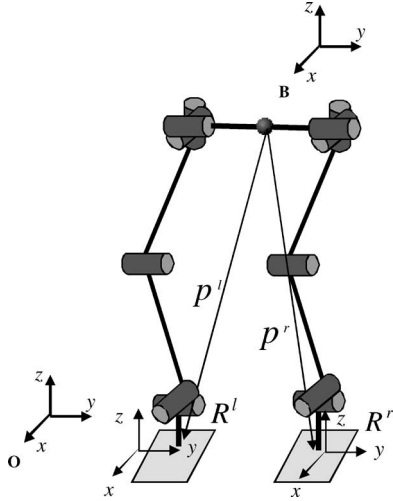


Fig. 2. Robot configuration.

Equation (1) states that the energy supplied to a passive network must be greater than negative $E(0)$ for all time [25].

The sampled time-passivity concept has been proposed recently in [26], because many of the input and output variables in control problems can be measured by computer, and the conjugate variables that define power flow in such a computer system are sampled time values. The robot control system to compensate for the landing force is assumed to take a force as an input, and computes foot's position as its output. Typically, this force input is measured by force sensors and used through A-D converter in each sample time. And the computed position output is applied to a motor controller so that motors can follow reference position continuously.

Following variables for force and position are defined during one sample time $t_{k-1} \leq t < t_k$ for the sampled time system.

- 1) $f(t) = F(t_k)$ is the force at k sample time.
- 2) $x(t_k)$ and $x(t_{k-1})$ are the position at k and $k - 1$ sample times, respectively.

Then, the passivity of the sampled system can be defined as follows.

Definition 2: The one-port network N with initial energy storage $E(0)$ is sampled time passive if and only if

$$E(t_k) = \sum_{j=0}^k F(t_j)(x(t_j) - x(t_{j-1})) + E(0) \geq 0 \quad (2)$$

where $j = 0, 1, 2, \dots, k = 0, 1, 2, \dots$, for sampled force $F(t_j)$ and position $x(t_j)$.

Note that, if $E(t_k) \geq 0$ for every k , the system dissipates energy, and if $E(t_k) < 0$, the system generates energy at time t_k .

III. ROBOT'S FOOT SYSTEM MODELING

Fig. 2 illustrates the robot's model and coordinates, where Σ_O is the global coordinates frame. We assume that the robot's center of gravity (COG) is at the midpoint of the hip joints, and define it as the origin of the body coordinate frame Σ_B . The position and posture of the robot's foot can be described with respect to this coordinate frame. 3-D vectors p^r and p^l represent the position of robot's right and left foot, respectively, and 3×3 matrices R^r and R^l represent the posture of robot's right and left foot, respectively. The foot's position p can be expressed as follows:

$$p^i = [x^i \quad y^i \quad z^i], \quad i \in \{r, l\}. \quad (3)$$

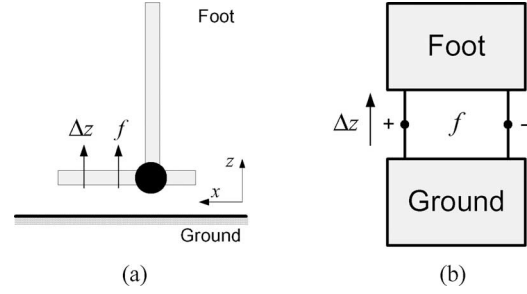


Fig. 3. Robot's foot system modeling. (a) Robot's foot and ground surface. (b) One-port network models of the robot's foot and ground surface.

To implement the time-domain passivity approach, the robot's foot and the ground are modeled as a network system. Both systems can be modeled as one-port network systems, which are connected to each other. The impedance of the ground is zero when the foot is in swing mode, and has a certain value when the foot is in contact with ground. Fig. 3(a) and (b) shows the real and the modeled network system, respectively. The sign convention for force and velocity is defined so that the energy is positive when the power enters the system port of the robot's foot. In Fig. 3(b), the force and the velocity are positive in the upper direction. Following Definition 2 and Fig. 3(b), and using time index j instead of t_j for notational simplicity, passivity of the robot's foot system can be described as

$$E(k) = \sum_{j=0}^k F(j)(z(j) - z(j-1)) + E(0) \quad (4)$$

$$= \sum_{j=0}^k F(j)\Delta z(j) + E(0) \geq 0 \quad (5)$$

where z is the height position of the foot in (3).

Since the ground can be considered as an intrinsically passive system, the connected system (the robot's foot and the ground) can be passive if the robot's foot, the one-port network, is passive. This is the case when the foot is physically absorbing the contact force. Once we prove the passivity, stability of the system can also be guaranteed because passivity is a sufficient condition of stability [21].

On the other hand, when the robot's foot, one-port network, is active (while the input energy is negative), the robot might be unstable. This is the case when the robot's foot kicks the surface, which causes a big landing force between the foot and the ground. This force can be a source for the unstable walking. Therefore, a control algorithm is required for alleviating the landing force.

IV. COMPENSATION FOR THE LANDING FORCE USING TIME-DOMAIN PASSIVITY CONTROL

A. Control Strategy for Foot's Landing

The biped robot periodically repeats the single-support phase and the double-support phase during walking. When the single-support phase is changed to double-support phase, the robot's foot starts to contact with ground surface. At this moment, the robot gets a big force that can make the robot unstable. To prevent this phenomenon, the contact phase should be inserted between swing phase and support phase.

Fig. 4 shows the sequence of biped walking phase. The contact phase begins with foot's landing on ground, and it can be sensed typically by force sensors that are mounted on the sole or ankle of the foot. When a

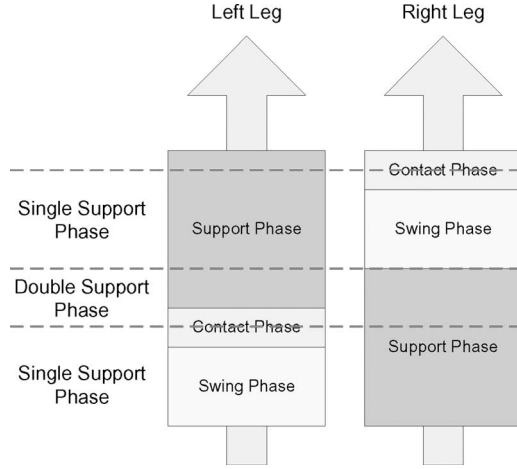


Fig. 4. Sequence of biped walking phases.

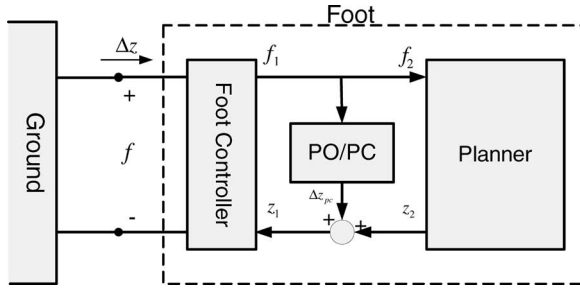


Fig. 5. One-port network of robot's foot with PO/PC.

walking trajectory is generated, it is usually expected that the contact phase begins with the end of the single-support phase and ends with the start of the double-support phase. However, it can begin during the single-support phase because of the uncertainty of ground level or the slight difference of two legs' length in real implementation. During the contact phase, the leg should absorb much of the force from the ground surface, and accept some portions of the robot weight. After controlling the landing force to stabilize the robot, the robot should be able to keep walking according to original walking trajectory. The legs support the weight of the robot and propel the robot's body in the double-support phase.

B. Landing Force Control

As shown in Fig. 5, the one-port network of the robot's foot system [Fig. 3(b)] can be divided into two parts, a foot position controller and a planner for generating the walking trajectory. The figure shows the overall network system of robot's foot along with a passivity control. The proposed time-domain passivity control consists of a passivity observer (PO) and passivity controller (PC), which respectively monitors and controls the input/output energy flow between the robot's foot and the ground. f ($=f_1 = f_2$) is the landing force, which can be measured by the force sensors on the robot's foot, z is the actual height position of the robot's foot, and Δz is the difference between two consecutive sampled data of z .

If the originally planned walking trajectory is employed, the robot's foot might get a big landing force from the ground in a very short time, and it makes the one-port of the robot's foot active. Thus, the modified foot position (z_1) is calculated from the originally planned trajectory (z_2), and the output of the PO/PC (Δz_{pc}). z_2 is a planned height position of walking trajectory from the planner without considering

the landing force from the ground. For alleviating the landing force, the PC is attached to modify the original walking trajectory (z_2) to z_1 by adding Δz_{pc} . Therefore, the robot takes the ground reaction force into account, and it can make a contact with the ground more securely.

PO computes the energy flow using the landing force and the foot position as follows:

$$W(k) = W(k-1) + f_1(k)(z_1(k) - z_1(k-1)) \quad (6)$$

$$W_o(k+1) = W(k) + f_1(k)(z_2(k+1) - z_1(k)) \quad (7)$$

where $W(k)$ is the total energy output from 0 to k , and $W_o(k+1)$ is the prediction of the one-step-ahead total energy output. The last term of (7) is the estimation of the one-step-ahead energy output, which is the output energy from k to $k+1$. Note that the planned position $z_2(k+1)$ is available at step k . If the PO can predict whether the system at the next step will be passive or not at the current step k , the PC can modify the desired position at the next step ($k+1$) to make the system passive. The PC absorbs exactly the net energy output, if any, measured by the PO at each time sample. Using the PO (steps 4 and 5 described next), the following PC algorithm is developed for the one-port robot's foot.

- 1) $f_1(k) = f_2(k)$ is the input.
- 2) $\Delta z_1(k) = z_1(k) - z_1(k-1)$
 $\Delta z_2(k+1) = z_2(k+1) - z_1(k)$.
- 3) $\Delta z_2(k)$ is the output of the one-port network.
- 4) $W(k) = W(k-1) + f_1(k)\Delta z_1(k)$ is the energy output at step k .
- 5) $W_o(k+1) = W(k) + f_1(k)\Delta z_2(k+1)$ is the prediction of the energy at step $k+1$.
- 6) The PC output for making the system passive is calculated as follows:

$$\Delta z_{pc} = \begin{cases} \frac{-W_o(k+1)}{f_1(k)}, & \text{if } W_o(k+1) < 0 \\ 0, & \text{if } W_o(k+1) \geq 0. \end{cases}$$

- 7) The stable boundary limits the PC output as follows:

$$\Delta z_{pc} = \Delta z_{pc_MAX}, \quad \text{if } \Delta z_{pc} > \Delta z_{pc_MAX}.$$

- 8) The modified desired height position [$z_1(k+1)$] is calculated from $\Delta z_1(k+1) = \Delta z_2(k+1) + \Delta z_{pc}(k)$.

The stable boundary Δz_{pc_MAX} , which considers robot's state such as size of a foot, weight of a leg, and walking speed, is used to restrict the PC output, because a sudden big change of the foot's position can influence the robot's stability. In step 7, a sudden change of the PC output is limited so that zero moment point (ZMP) can stay within a desired stable region during the landing force control [13].

This method can obtain the foot's position to reduce the landing force from simple computation without any knowledge of the system. Because PC injects the adaptive damping whenever net energy is produced, it is also able to work properly in wide variety of operating conditions. Moreover, the stability of the proposed force control system can be guaranteed by passivity property.

C. Recover to the Original Trajectory

Once the stable landing is achieved, the robot's walking trajectory should be modified to follow the originally planned walking trajectory [27]. To solve the problem, a mass-concentrated robot model is considered. The equation of motion in vertical direction is expressed as follows:

$$m(\ddot{z}_G + g) = f$$

$$\ddot{z}_G = \frac{f}{m} - g \quad (8)$$

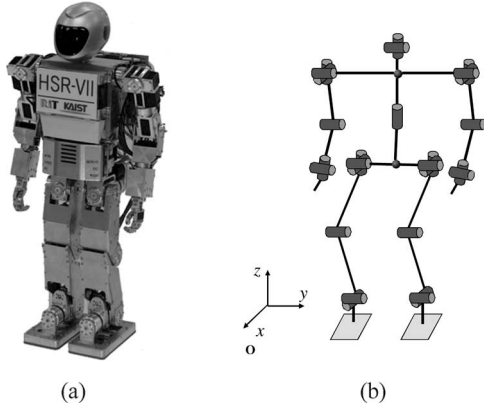


Fig. 6. Small-sized humanoid robot: HanSaRam-VII. (a) HanSaRam-VII. (b) Configuration.

where z_G is the COG relative to the global coordinate system in the z -axis, m is the total mass of the robot, and g is the acceleration of gravity. In sampled time system, (8) becomes

$$\Delta z_G(k+1) = \Delta z_G(k) + \left(\frac{f(k)}{m} - g \right) T^2 \quad (9)$$

with

$$\Delta z_G(k) \equiv z_G(k) - z_G(k-1)$$

where T is the sampling time. In order to recover the COG to the desired position, an error compensation is added as follows:

$$\begin{aligned} \Delta z_G(k+1) = & \Delta z_G(k) + \left(\frac{f(k)}{m} - g \right) T^2 \\ & + K \Delta^{\text{ref}} z_G(k) + D \Delta^2 z_G(k) \end{aligned} \quad (10)$$

with

$$\Delta^{\text{ref}} z_G(k) \equiv z_G^{\text{ref}}(k) - z_G(k)$$

$$\Delta^2 z_G(k) \equiv \Delta^{\text{ref}} z_G(k) - \Delta^{\text{ref}} z_G(k-1)$$

where z_G^{ref} is a reference value, and K and D are the proportional and the differential gain, respectively.

After the stable landing, the force f is equal to the weight of the robot (mg), and also it means $\ddot{z}_G = 0$. As a result, the motion to follow the original trajectory can be obtained as follows:

$$\Delta z_G(k+1) = \Delta z_G(k) + K \Delta^{\text{ref}} z_G(k) + D \Delta^2 z_G(k). \quad (11)$$

In this stage, PO is also reset to prepare the next observation.

V. EXPERIMENTS

A. Experimental System Description

Fig. 6 shows the small-sized humanoid robot, HanSaRam-VII. Its height and weight are 50 cm and 5.3 kg, respectively. It has 27 DOFs, and consists of 13 dc motors with harmonic drives for reduction gears in the lower body and 16 RC servo motors (two servo motors in each hand control, 1 DOF per hand) in the upper body. The onboard Pentium-III-compatible PC, running RT-Linux, calculates the walking trajectory in real time. The walking trajectory is generated online through 3-D inverted pendulum mode [28]. To measure forces on the foot, four force sensing resistors (FSRs) are equipped on each foot's sole.

The proposed time-domain passivity control is implemented as shown in Fig. 7. During the swing and the support phases, the robot's

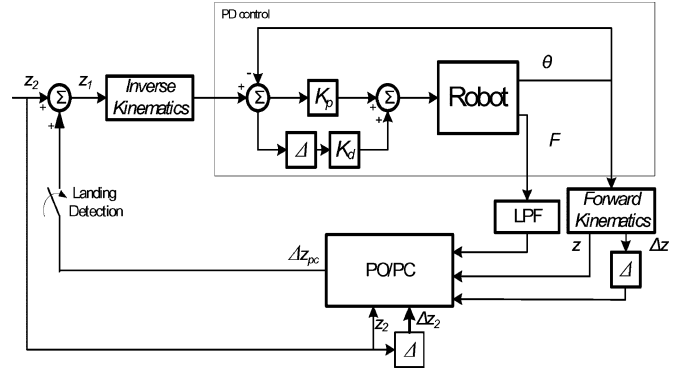


Fig. 7. Time-domain passivity control system of HanSaRam-VII.

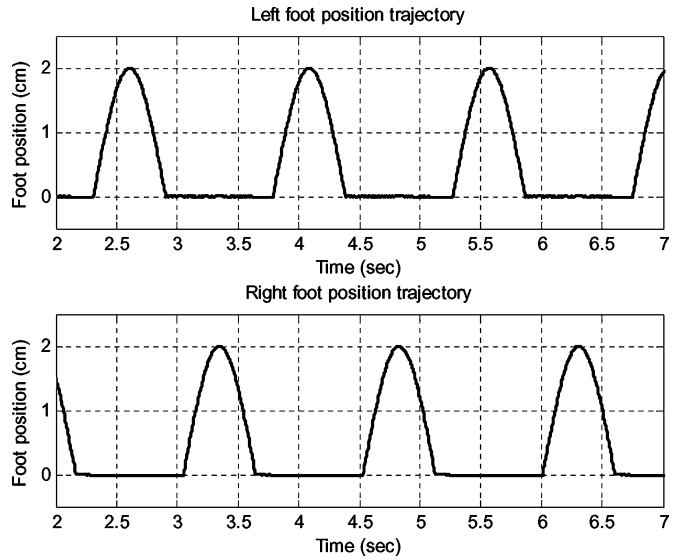


Fig. 8. Foot's height position trajectories without landing force control.

legs are controlled by potential difference (PD) control to follow the desired trajectory that is calculated in the walking trajectory planner. K_p and K_d are coefficients of the PD controller, and Δ represents a difference operation between two consecutive sampled data. A low-pass filter (LPF) is used to get reliable force value, because the measured value from FSR sensors have high-frequency noises. If landing moment is detected from FSR sensors, the robot's leg will be in the contact phase, and then, immediately, the PO/PC compensates for the landing force. This computed position is added to the originally planned foot's position, which is used for inverse kinematics. PD controller controls the motors in low level to follow the modified position.

B. Experimental Results

Dynamic walking experiments were performed to verify the proposed time-domain passivity control approach. The results are compared with those using no landing force control and the damping control to absorb the landing force. In the experiments, the biped robot walked with a speed of 5.3 cm/s and a step length of 4.0 cm. Double- and single-support phases of a step were 0.15 and 0.60 s, respectively. The contact phase started when the foot landed on ground surface. All experimental results are plotted after the initial 2 s of operation, and then, for 5 s thereafter.

1) *Walking Experiments Without Landing Force Control*: First, the experiments were performed without landing force control. Fig. 8

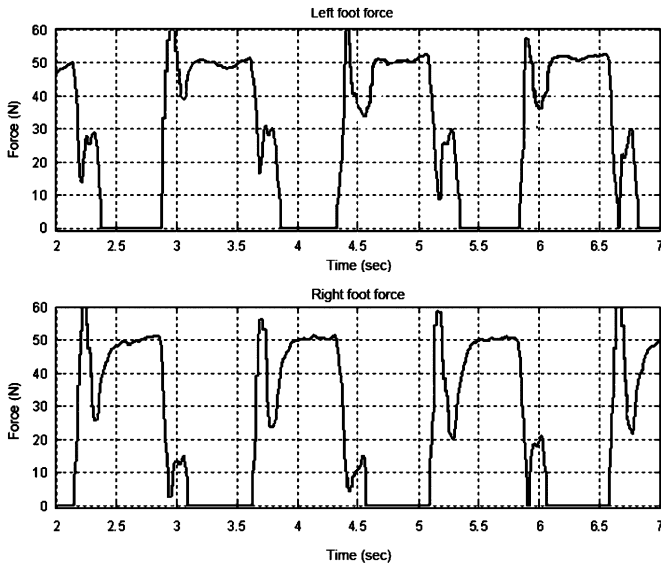


Fig. 9. Force (f) without landing force control.

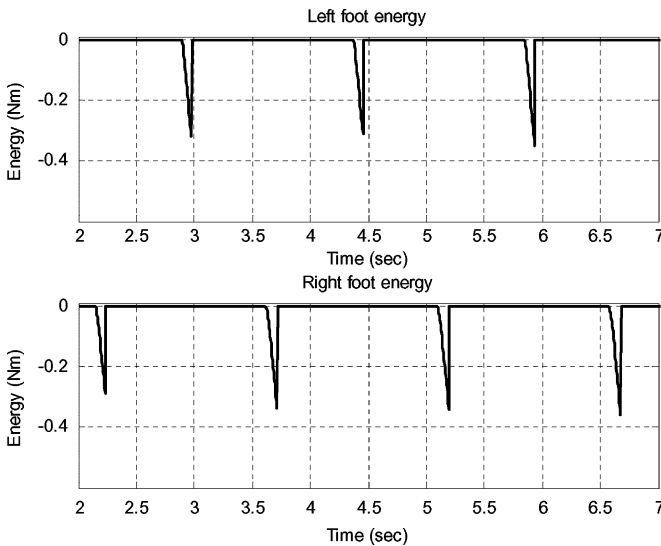


Fig. 10. Energy (W) without landing force control.

shows the foot's height position trajectories, which was the output of the walking pattern generator without considering landing force. The foot's position is plotted in global coordinate frame so that the position 0 means the ground surface level. When robot's foot was landing, there was a big landing force, as shown in Fig. 9. The maximum value of the left foot's force was 62.84 N, and it was 1.21 times the robot's weight. This force caused "double contacts" of the foot. Even after the robot's foot landed on the ground, it was bounced back from the ground instantaneously due to the big landing force such that it disturbed stable dynamic walking. The repulsive force accelerated robot's COG, and made the robot to hop pouncingly. During the support phase, there were two large peaks at the start and end of supporting time. The first peak was caused by the foot's landing at the beginning of the double-support phase, and the second peak came from the another foot's landing at the start of the next double supporting phase. It should be noted that two force plots are different because the mass distribution was asymmetric in the real robot. Fig. 10 shows the input energy from the one-port robot's foot. When the foot kicks the surface, the energy becomes neg-

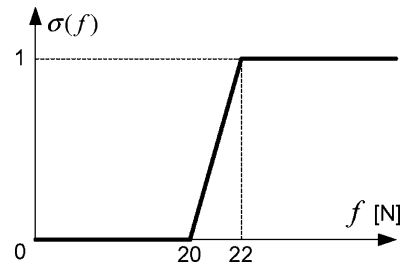


Fig. 11. Switching function for the damping control method.

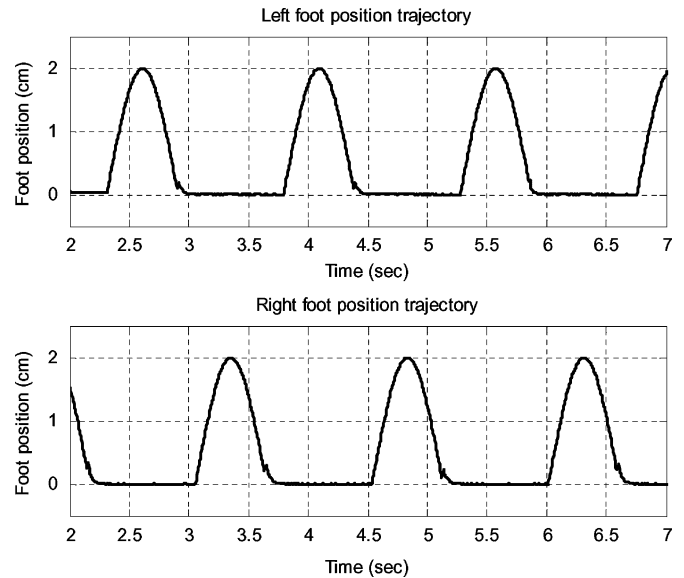


Fig. 12. Foot's height position trajectories by the damping control method.

ative, and the robot's foot is no longer passive. It means that the robot might be unstable due to this active energy output from the foot system.

2) *Walking Experiments by the Damping Control Method:* In the second experiments, the controller made the robot shorten the contacting legs when the huge landing force was detected as [14]

$$\Delta \dot{z}_d = \sigma(f)v + (1 - \sigma(f))(-\omega \Delta z_d) \quad (12)$$

where Δz_d is the modification of the foot height and f is the landing force. The control mode was switched by the function of $\sigma(f)$ (Fig. 11). In the experiments, v and ω were selected as 15 and 32, respectively.

Fig. 12 shows that the foot was moved a little bit upward to absorb the landing force. The modification of the foot's position is plotted in Fig. 13. Fig. 14 indicates that the landing force was reduced relatively in comparison with the previous result. The maximum peak value of the right foot's force at landing was 20.45 N. But, from the energy viewpoint, it is not enough to meet the passive condition, as shown in Fig. 15. The control system was still active. Though the damping control method could reduce the force somewhat, it was too difficult to obtain a reasonable control parameters [v , ω , and $\sigma(f)$] for the experiments. For example, if ω was increased to move the foot more upward for absorbing landing force, the robot could not walk due to the leg's big motion. However, when ω was selected to be of lower value to walk, the landing force could not be reduced as much as it was desired. In addition to that, if this fixed damping control is employed in the different environment such as different walking speed or different foot's height, the parameters should be changed or regulated properly according to the environment, in order to work well.

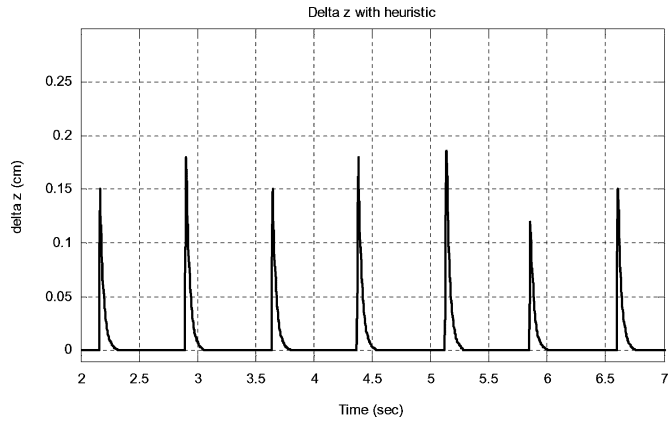


Fig. 13. Modification of the foot's position (Δz_d) by the damping control method.

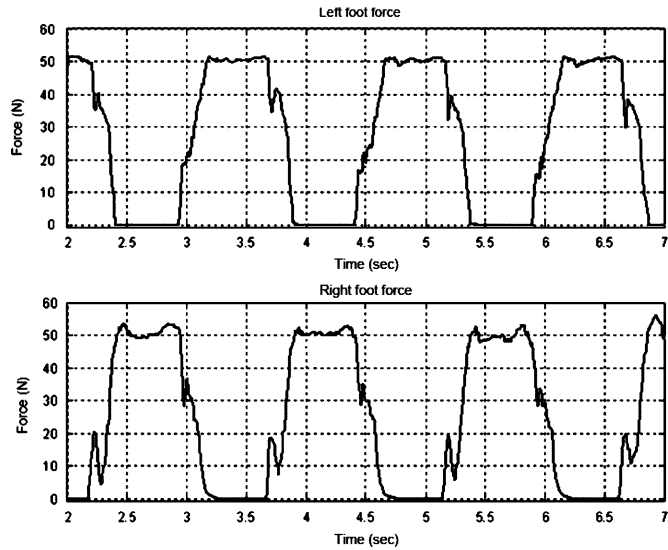


Fig. 14. Force (f) by the damping control method.

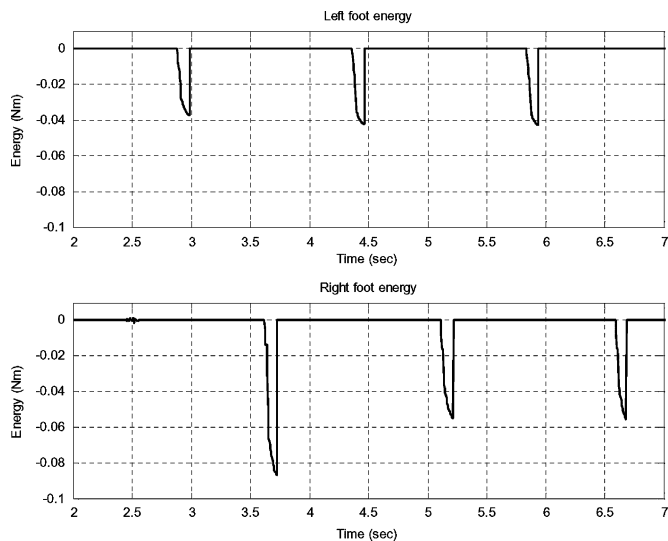


Fig. 15. Energy (W) by the damping control method.

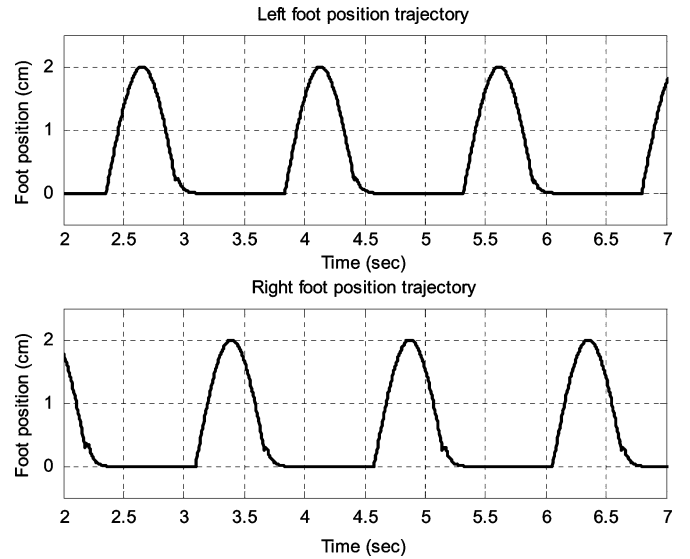


Fig. 16. Foot's height position (Δz_1) trajectories by the PO/PC method.

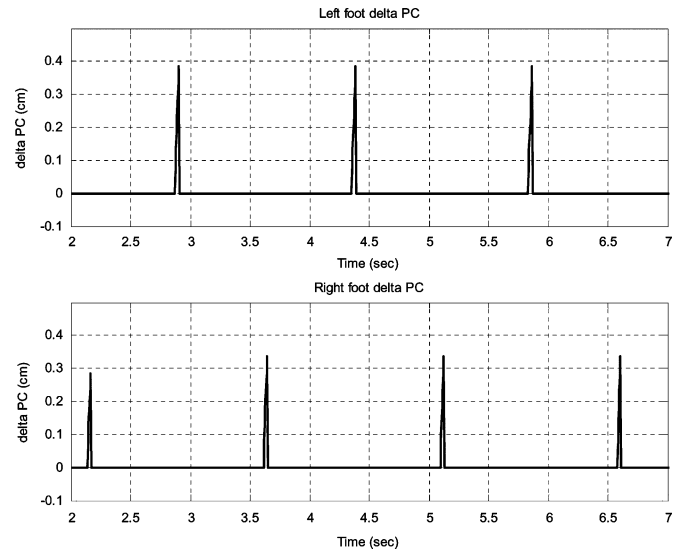
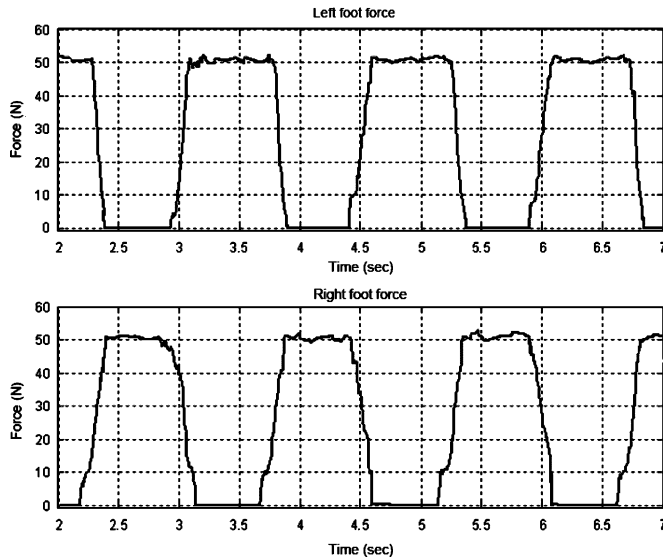
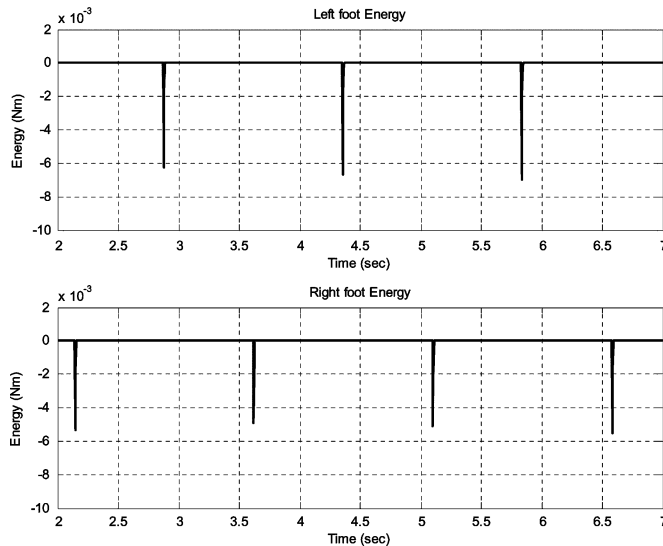


Fig. 17. Output of PO/PC (Δz_{pc}) by the PO/PC method.

3) *Walking Experiments by the PO/PC Method:* Figs. 16–19 show the results when the proposed time-domain passivity approach was applied. Figs. 16 and 17 show the foot's height position (z_1) trajectories by the proposed passivity method and the output of the PO/PC (Δz_{pc}), respectively.

Foot was slightly moved upward on each landing time, since the PC modified the desired foot position to satisfy the passivity condition, and the output of the PO/PC was varied according to its energy. Compared with the damping control method that used fixed parameters, the proposed control showed better performance. Since the adaptive damping element is injected by the PO/PC, it can be used in wide dynamic environment range. As shown in Fig. 18, the foot landed on the ground surface without impact forces, because the PC immediately absorbed them. There was no presence of "double contact" any more. Fig. 19 shows the robot system's energy while walking. Due to the bigger force than the value that PO initially estimated, the system could not be passive at the landing time. But the system was controlled to satisfy the passivity condition by five steps (25 ms), and the figure shows the

Fig. 18. Force (f) by the PO/PC method.Fig. 19. Energy (W) by the PO/PC method.

scale of negative energy was decreased by 10–100 times compared to the other previous results (Figs. 10 and 15).

Fig. 20 represents ZMP trajectories relative to the global coordinate system. The size of the rectangle that represents the foot placement is 4 cm \times 6 cm. Without landing force control, the deviation of the ZMP position from the desirable ZMP position (the center of the foot) was bigger than those of other methods. “Double contact” at the landing time even caused the ZMP to jump to the boundary of the foot. However, when the proposed method was used, the deviation of the ZMP from its desirable position was small compared to other methods. Thus, it can be concluded that the proposed method enhances the stability of the robot during walking.

The results of the overall experiments indicate that the proposed controller decreases the impulsive landing force at the ground surface and makes stable foot landings possible. System dynamic equations are not used anywhere in the proposed method, and control parameters for the PO/PC are not required at all. Also note that the proposed method is not limited to small-sized robots.

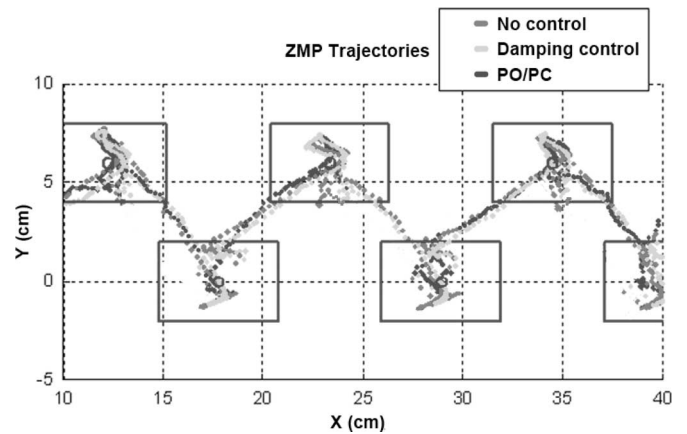


Fig. 20. ZMP trajectories.

VI. CONCLUSION

This paper proposed a new method to compensate for the landing force of a humanoid robot. For the use of the time-domain passivity approach, the ground and the robot’s foot were modeled as two one-port network systems, which were connected, and exchanged energy with each other. Time-domain passivity control, which has the landing force as an input and foot’s height position as an output, was implemented. The proposed control algorithm does not require complex dynamic equations and parameter adjustment for control scheme. The damping element in the proposed method can also be adaptively adjusted so that it can be used in the dynamic environment. Moreover, the stability of the force control system can be obtained by passivity property. The effectiveness of the proposed method was demonstrated by carrying out real experiments with the developed small-sized humanoid robot, HanSaRam-VII.

REFERENCES

- [1] K. Hirai, M. Hirose, Y. Haikawa, and T. Takenaka, “The development of Honda humanoid robot,” in *Proc. IEEE Int. Conf. Robot. Autom.*, Leuven, Belgium, May 1998, pp. 1321–1326.
- [2] Y. Ogura, Y. Sugahara, Y. Kaneshima, N. Hieda, H.-O. Lim, and A. Takanishi, “Interactive biped locomotion based on visual/auditory information,” in *Proc. IEEE Int. Workshop Robot Human Interactive Commun.*, Berlin, Germany, Sep. 2002, pp. 253–258.
- [3] S. Kagami, K. Nishiwaki, J. J. Kuffner, Y. Kuniyoshi, M. Inaba, and H. Inoue, “Online 3D vision, motion planning and bipedal locomotion control coupling system of humanoid robot: H7,” in *Proc. IEEE Int. Conf. Intell. Robots Syst.*, vol. 3, Lausanne, Switzerland, Oct. 2002, pp. 2557–2562.
- [4] J.-H. Kim, D.-H. Kim, Y.-J. Kim, K.-H. Park, J.-H. Park, C.-K. Moon, K. T. Seow, and K.-C. Koh, “Humanoid robot HanSaRam: Recent progress and development,” *J. Adv. Comput. Intell. Intell. Inf.*, vol. 8, no. 1, pp. 45–55, Jan. 2004.
- [5] S. Setiawan, S. Hyon, J. Yamaguchi, and A. Takanishi, “Physical interaction between human and a bipedal humanoid robot,” in *Proc. IEEE Int. Conf. Robot. Autom.*, vol. 1, Detroit, MI, May 1999, pp. 361–367.
- [6] K. Harada, S. Kajita, F. Kanehiro, K. Fujiwara, K. Kaneko, K. Yokoi, and H. Hirukawa, “Real-time planning of humanoid robot’s gait for force controlled manipulation,” in *Proc. IEEE Int. Conf. Robot. Autom.*, vol. 1, New Orleans, LA, Apr. 2004, pp. 616–622.
- [7] S. Kajita, A. Kobayashi, and T. Yamamura, “Dynamic walking control of a biped robot along a potential energy conserving orbit,” *IEEE Trans. Robot. Autom.*, vol. 8, no. 4, pp. 431–438, Aug. 1992.
- [8] Q. Huang, K. Yokoi, S. Kajita, K. Kaneko, H. Arai, N. Koyachi, and K. Tanie, “Planning walking patterns for a biped robot,” *IEEE Trans. Robot. Autom.*, vol. 17, no. 3, pp. 280–289, Jun. 2001.
- [9] K. Nishiwaki, S. Kagami, Y. Kuniyoshi, M. Inaba, and H. Inoue, “Online generation of humanoid walking motion based on a fast generation

- method of motion pattern that follows desired ZMP," in *Proc. IEEE/RSJ Int. Conf. Intell. Robots Syst.*, vol. 3, Lausanne, Switzerland, Sep. 2002, pp. 2684–2689.
- [10] J. Yamaguchi, E. Soga, S. Inoue, and A. Takanishi, "Development of a bipedal humanoid robot control method of whole body cooperative dynamic biped walking," in *Proc. IEEE Int. Conf. Robot. Autom.*, vol. 1, Detroit, MI, May 1999, pp. 368–374.
- [11] M. Popovic, A. Hofmann, and H. Herr, "Zero spin angular momentum control: Definition and application," in *Proc. IEEE/RSA Int. Conf. Humanoid Robots*, vol. 1, Los Angeles, CA, Nov. 2004, pp. 478–493.
- [12] B.-J. Lee, Y.-D. Kim, and J.-H. Kim, "Balance control of humanoid robot for hurosot," presented at the IFAC World Congr., Prague, Czech Republic, Jul. 2005.
- [13] Q. Huang and Y. Nakamura, "Sensory reflex control for humanoid walking," *IEEE Trans. Robot. Autom.*, vol. 21, no. 5, pp. 997–984, Oct. 2005.
- [14] S. Kajita, T. Nagasaki, K. Kaneko, K. Yokoi, and K. Tanie, "A running controller of humanoid biped HRP-2LR," in *Proc. IEEE Int. Conf. Robot. Autom.*, Barcelona, Spain, Apr. 2005, pp. 618–624.
- [15] J. Yamaguchi, N. Kinoshita, A. Takanishi, and I. Kato, "Development of a dynamic biped walking system for humanoid development of a biped walking robot adapting to the humans' living floor," in *Proc. IEEE Int. Conf. Robot. Autom.*, vol. 1, Minneapolis, MN, Apr. 1996, pp. 232–239.
- [16] F. Silva and J. Machado, "Position/force control of biped walking robots," in *Proc. IEEE Int. Conf. Syst., Man, Cybern.*, vol. 5, Nashville, TN, Oct. 2000, pp. 3288–3293.
- [17] M. Shibata and T. Natori, "Impact force reduction for biped robot based on decoupling COG control scheme," in *Proc. IEEE Int. Workshop Adv. Motion Control*, Nagoya, Japan, Apr. 2000, pp. 612–617.
- [18] J.-H. Park, "Impedance control for biped robot locomotion," *IEEE Trans. Robot. Autom.*, vol. 17, no. 6, pp. 870–882, Dec. 2001.
- [19] H.-O. Lim, S. Setiawan, and A. Takanishi, "Position-based impedance control of a biped humanoid robot," *Adv. Robot.*, vol. 18, no. 4, pp. 415–435, 2004.
- [20] J. Yamaguchi, A. Takanishi, and I. Kato, "Development of a biped walking robot compensating for three-axis moment by trunk motion," in *Proc. IEEE/RSJ Int. Conf. Intell. Robots Syst.*, vol. 1, Yokohama, Japan, Jul. 1993, pp. 561–566.
- [21] B. Hannaford and J.-H. Ryu, "Time-domain passivity control of haptic interfaces," *IEEE Trans. Robot. Autom.*, vol. 18, no. 1, pp. 1–10, Feb. 2002.
- [22] J.-H. Ryu, D.-S. Kwon, and B. Hannaford, "Stability guaranteed control: Time domain passivity approach," *IEEE Trans. Control Syst. Technol.*, vol. 12, no. 6, pp. 860–868, Nov. 2004.
- [23] Y.-D. Kim, B.-J. Lee, J.-K. Yoo, J.-H. Kim, and J.-H. Ryu, "Compensation for the landing impact force of a humanoid robot by time domain passivity approach," in *Proc. IEEE Int. Conf. Robot. Autom.*, Orlando, FL, May 2006, pp. 1225–1230.
- [24] Y.-D. Kim, B.-J. Lee, J.-K. Yoo, J.-H. Kim, and J.-H. Ryu, "Landing force controller for a humanoid robot: Time-domain passivity approach," in *Proc. IEEE Int. Conf. Syst., Man, Cybern.*, Taipei, Taiwan, Oct. 2006, pp. 4237–4242.
- [25] A. J. van der Schaft, *L2-Gain and Passivity Techniques in Nonlinear Control* (Communications and Control Engineering Series). Berlin, Germany: Springer-Verlag, 2000.
- [26] J.-H. Ryu, Y.-S. Kim, and B. Hannaford, "Sampled- and continuous-time passivity and stability of virtual environments," *IEEE Trans. Robot.*, vol. 20, no. 4, pp. 772–776, Aug. 2004.
- [27] T. Sugihara and Y. Nakamura, "Whole-body cooperative balancing of humanoid robot using COG jacobian," in *Proc. IEEE/RSJ Int. Conf. Intell. Robots Syst.*, vol. 3, Lausanne, Switzerland, Sep. 2002, pp. 2575–2580.
- [28] S. Kajita, F. Kanehiro, K. Kaneko, K. Fujiwara, K. Yokoi, and H. Hirukawa, "Biped walking pattern generation by a simple three-dimensional inverted pendulum model," *Adv. Robot.*, vol. 17, no. 2, pp. 131–147, 2003.